



University of Kentucky
UKnowledge

KWRRI Research Reports

Kentucky Water Resources Research Institute

10-1971

Detection and Identification of Molecular Water Pollutants by Laser Raman Spectroscopy

Digital Object Identifier: <https://doi.org/10.13023/kwrri.rr.44>

Eugene B. Bradley
University of Kentucky

Charles A. Frenzel
University of Kentucky

John Reeves
University of Kentucky

Robert McConnell
University of Kentucky

Kay Lane
University of Kentucky

Right click to open a feedback form in a new tab to let us know how this document benefits you.

Follow this and additional works at: https://uknowledge.uky.edu/kwrri_reports

 Part of the [Water Resource Management Commons](#)

Repository Citation

Bradley, Eugene B.; Frenzel, Charles A.; Reeves, John; McConnell, Robert; and Lane, Kay, "Detection and Identification of Molecular Water Pollutants by Laser Raman Spectroscopy" (1971). *KWRRI Research Reports*. 151.
https://uknowledge.uky.edu/kwrri_reports/151

This Report is brought to you for free and open access by the Kentucky Water Resources Research Institute at UKnowledge. It has been accepted for inclusion in KWRRI Research Reports by an authorized administrator of UKnowledge. For more information, please contact UKnowledge@lsv.uky.edu.

DETECTION AND IDENTIFICATION OF MOLECULAR WATER
POLLUTANTS BY LASER RAMAN SPECTROSCOPY

Dr. Eugene B. Bradley
Principal Investigator

Charles A. Frenzel
Research Engineer

Graduate Student Assistant: John Reeves
Robert McConnell
Kay Lane

Project Number A-015-KY (Completion Report)
Agreement Number 14-31-0001-3217
Period of Project September 1968 - August 1971

University of Kentucky Water Resources Institute
Lexington, Kentucky

The work on which this report is based was supported in part by funds provided by the Office of Water Resources Research, United States Department of the Interior, as authorized under the Water Resources Research Act of 1964.

October 1971

ABSTRACT

Laser Raman spectroscopy is evolving into a primary tool for the identification of molecular water pollutants. This study pushes the limits of detectivity of carbon disulfide and benzene to ~ 20 ppm in water solutions using a high-resolution Raman spectrometer, cooled detectors, and photon counting techniques. The primary limiting factors were found to be the low throughput and the scattered light performance of the monochromator as well as insufficient laser energy.

An optimized design for a pollution-measuring instrument is suggested, and a prototype has been built which is useful with any value of excitation energy short of sample degrading. The present instrument scans spectrum windows with fixed preselecting filters followed by a small single monochromator with high throughput. No detector cooling or refinements in signal processing were attempted. The resulting detectivity with 20 mw of laser power was only 1000 ppm. However, the scattered light background or "optical noise" is unmeasurable except at the laser frequency, where it was a maximum of six percent of full scale measured against the 992 cm^{-1} Raman band of benzene. Equipped with an ion laser a practical field instrument capable of detectivity of 1 ppm will cost about \$20,000. The instrument described herein can be built for \$4,000, less laser.

KEY WORDS

(a) Pollutant identification, (b) Measuring instruments, (c) Spectrometers, (d) Laser, (e) Raman

TABLE OF CONTENTS

	Page
ABSTRACT	ii
LIST OF TABLES	iv
LIST OF ILLUSTRATIONS	v
CHAPTER	
I INTRODUCTION	1
II RESEARCH PROCEDURES	17
1. Solutions	17
2. Instrument Function	17
III DATA AND RESULTS	19
Laser Raman Spectrometer	31
IV CONCLUSIONS	39
REFERENCES	40

LIST OF TABLES

Table		Page
I	A Comparison of Raman Band-Intensity- Proportional Parameters for the 1028 cm^{-1} Raman Band of CH_3OH and the 458 cm^{-1} Raman Band of CCl_4	22
II	Ratios of Raman Band Widths at Three Spectral Slit Widths	23
III	A Codification of Two Raman Bands of CH_3OH According to F-Values	24

LIST OF ILLUSTRATIONS

Figure		Page
1	Spectral Attenuation Coefficients for Water From Various Geographical Locations	4
2	The Raman Spectrum of Distilled Water	6
3	A Portion of the Raman Spectrum of 50 ppm by Volume of Benzene in Distilled Water	7
4	Sketch of a Hypothetical Raman Band Divided Along the Band Center, B_c	20
5	The Normalized Band Half-Width of the CCl_4 Raman Band at 458 cm^{-1} and the Neon Emission Line at 6506.53 \AA for Various Slit Widths	21
6	The Normalized Band Half-Width of the CH_3OH Raman Band at 1028 cm^{-1} and the Neon Emission Line at 6717.04 \AA for Various Slit Widths	26
7	A Symmetry Plot of the Raman Band of CCl_4 at 458 cm^{-1} for Three Mechanical Slit Widths of the LR-1	27
8	The Corrections to Widths of the CCl_4 Raman Band at 458 cm^{-1} for Various Percentages of the Peak Height of the Band	28
9	Result of the Corrections to Bandwidth and Band Shape for the CH_3OH Raman Band at 1028 cm^{-1}	29
10	Typical Spectral Window Produced by a Band-Pass	33
11	Spectral Window Produced by the Filter in Fig. 10.	34
12	The 458 cm^{-1} Raman Band of CCl_4 Recorded on the Constructed Spectrometer	35
13	The 992 cm^{-1} Raman Band of C_6H_6 Recorded on the Constructed Spectrometer	36
14	Block Diagram of a Prototype Laser Raman Spectrometer	37

from which the complex molecular mixtures must be inferred, while GLC is limited to molecules of relatively low mol. wt. Infrared spectroscopy is not useful in this problem because of the strong absorption of water in that spectral region. However, Raman spectroscopy does not suffer from any of these limitations. Rather, it may offer a direct method of detection and identification of molecules in water solution or suspension because the Raman spectrum of distilled water is quite weak.

The Raman spectrum yields information which is complementary to i. r. data concerning molecular vibrations. The influence of molecular symmetry upon the quantum mechanical selection rules is such that the Raman and i. r. selection rules differ, i. e. molecular vibrations may be allowed in the Raman spectrum but forbidden in the i. r. spectrum and vice versa. Each type of molecule, therefore, possesses a unique signature through its Raman spectrum.

Until recently, the applicability of Raman spectroscopy to weak solution studies (which are of interest to water pollution analysts) was limited by the low spectral brightness of mercury-arc lamps used to excite the Raman spectra. However, the use of a gas laser eliminates the problem of low spectral brightness. The coherency of the laser light, its high degree of polarization, and its near-perfect beam collimation excite a quality of Raman spectra which was unattainable previously. The highly monochromatic character of a laser exciting source improves the ability to record Raman lines which occur close to the exciting laser line, making it possible to record low-frequency vibrational modes of large and/or heavy molecules. Also, Raman lines which are generated by symmetric molecular vibrations are polarized, and it is relatively easy to determine experimentally the degree of polarization. Thus the polarization characteristics of Raman lines may be useful as a tool by water pollution analysts as a further diagnostic technique to identify unknown molecular species in water samples.

Reported here are projected levels of detectivity of pollutants in water. In addition to these studies, work is reported on the effect of the slit function of the monochromator upon band width and band shape for Raman bands of

liquids. Such work prepares the way for measurement of volume concentration from intensity measurements of the Raman bands.

This work was performed using two Helium-Neon lasers of output powers 5 mw and 50 mw. Such lasers are not the ideal source for such work because the frequency (6328 Å) is not the frequency at which the attenuation coefficient for water is a minimum (see Fig. 1)*. Rather a high-power Argon ion laser would be the ideal Raman source for such investigation. One may expect detectivities of 1-5 ppm of molecular pollutants in water. With a pulsed source and digital recording techniques, detectivities of less than 1 ppm should be possible.

The Raman studies were initiated using a Perkin-Elmer Model LR-1 laser Raman spectrometer. All Raman spectra were obtained using a Perkin-Elmer 2.5 ml Raman sample cell. Several electronic and optical modifications were made in the Model LR-1 in order to enhance the recording sensitivity of the instrument. These modifications are summarized as follows.

(a) The original Perkin-Elmer 3m W He-Ne gas laser was replaced with a Spectra-Physics Model 120 5m He-Ne gas laser A 10 Å half bandwidth transmission filter centered about 6328 Å, the exciting line, was installed on the Spectra-Physics laser.

(b) Beam focusing lenses have been installed so that the exciting laser beam may be focused to a diameter of approximately 50 μ.

(c) A polarization scrambler has been constructed and placed before the entrance slit to eliminate preferential polarization by the monochromator optics.

(d) Slit width-spectral slit width curves have been obtained in order that the optimum signal-to-noise ratio may be determined. Neon emission lines were used to calibrate the spectral slit width.

*"Theoretical and Experimental Study of the Transmission of Laser Radiation Through Water," K. R. Hessel et. al., Texas University, Austin, Texas, May, 1969. Obtainable from Clearinghouse for Federal Scientific and Technical Information, PB184-114.

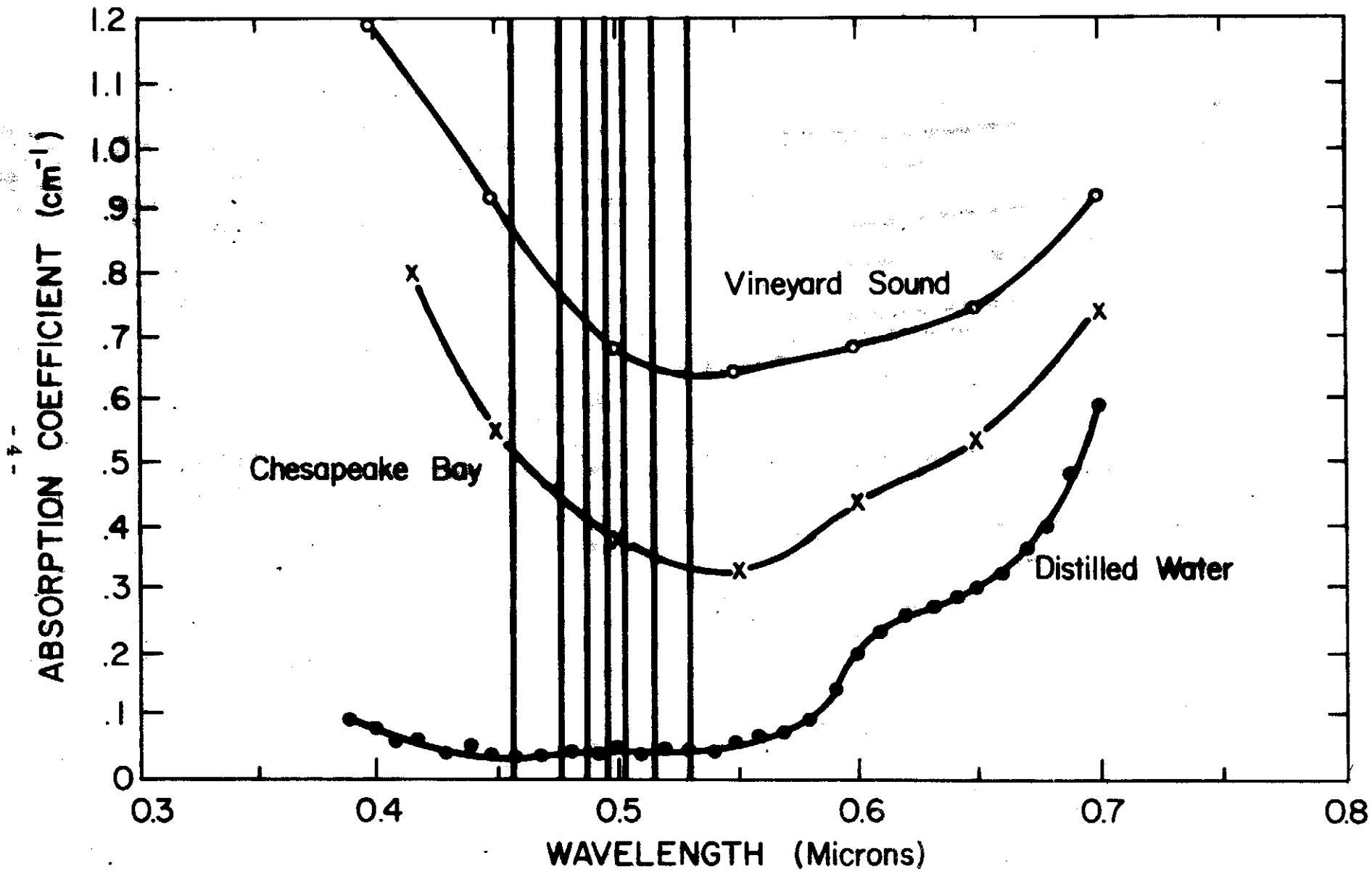


FIG. 1 Spectral Attenuation Coefficients for Water From Various Geographical Locations (after Hessel *et al.*)*

(e) Stacked, precalibrated Nikon neutral-density filters have been purchased for the attenuation of the Rayleigh-scattered light at the exciting wavelength.

(f) The photomultiplier tube is cooled with boil-off from a dewar of liquid nitrogen in order to reduce tube noise.

(g) A model 410 Jarrell-Ash 1/4 meter Ebert monochromator is used after the exit slit of the RL-1 to reduce scattered light.

(h) A new scan motor has been installed to permit slow scan speeds. The motor is reversible so that band shape analysis may be done by scanning in both the forward and reverse directions. Such a procedure is necessary to eliminate any instrumental or electronic distortion of the Raman band shape.

(i) A Keithley Model 300 operational amplifier used in the linear current amplifier mode has been purchased and installed as a preamplifier for the recording electronics.

(j) Additional filtering has been added to the existing phase-locked amplifier system to increase the recording time constant if desired.

The Raman spectrum of distilled water is shown for reference in Fig. 2. That laser Raman spectroscopy may be of value in the detection and the identification of molecular pollutants in water is shown in Fig. 3. The ability to detect 50 ppm of benzene in distilled water with only 5 mW of laser power output indicates that it should be possible to detect 10-20 ppm of molecular pollutants in water with 50 mW of laser output power at 6328 Å. Such an extrapolation was confirmed on a Jarrell-Ash Model 25-300 laser Raman spectrometer, equipped with a 50 mW He-Ne laser. With improved excitation techniques and 50 mW laser power, it may be possible to detect certain pollutants of fewer than 5 ppm with He-Ne lasers. The molecular type may be identified from knowledge of the frequencies and the polarizations of the Raman bands. The laser Raman spectrum of distilled water is weak and uncomplicated - thus it is possible to detect to distinguish Raman bands of pollutants in natural water from those of natural water. Laser Raman spectrometers may be constructed for field use by technicians. Such field

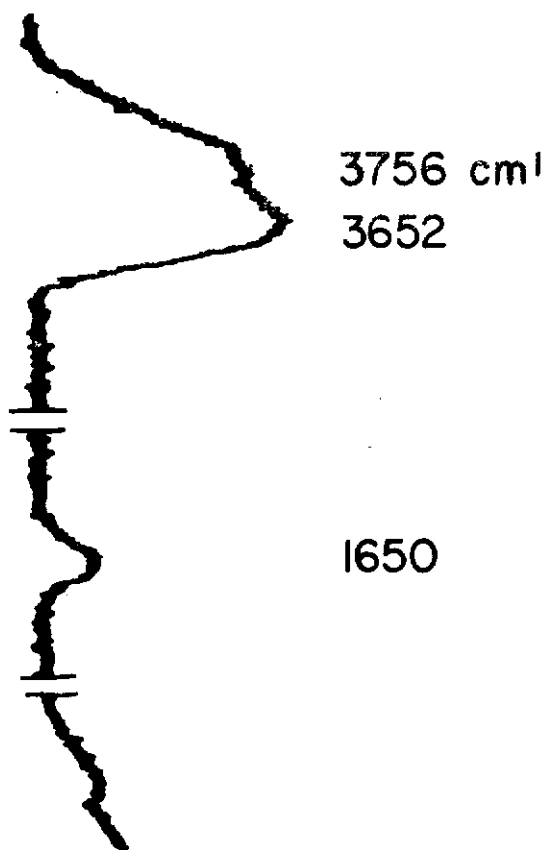


FIG. 2 The Raman Spectrum of Distilled Water. The Spectrum was Excited Using a 5 mw He-Ne Laser, 6328 Å. Slit Width 10 cm⁻¹, Recording Time 1 hr. Range 0-4000 cm⁻¹.



FIG. 3 A Portion of the Raman Spectrum of 50 ppm by Volume of Benzene in Distilled Water. The Raman Band at 992 cm^{-1} is the C-C Stretching Vibration, ν_2 , Slit Width 10 cm^{-1} , Recording Time 20 min.

instruments could be constructed to yield only certain Raman bands of pre-determined molecular pollutants, or a large frequency coverage with high sensitivity (higher cost) may be desirable for use at a regional monitoring office or at a 'standards' office. An example of a field instrument was constructed and tested for a cost of \$4,000, less laser. The description of this instrument is included in the last part of this report. However, before such an instrument is explained, there will be a discussion of some factors which affect the recorded intensity of Raman bands of liquids.

If the incident light is plane polarized with its electric vector at right angles to the direction of scattering the observed intensity is

$$(I_{\rho})_{\text{obs}} = \frac{KI_o(\nu_o - \nu)^4}{M\nu(1 - e^{-\frac{h\nu}{Kt}})} \left[45(\alpha')^2 + 7(r')^2 \right]$$

where

- K = constant
- r', α' = invariants of a derived tensor
- M = reduced mass

The intensity observed in practice will be proportional to the total number of scattering molecules in the sample. For a species in solution this fact implies proportionality to the volume concentration. However, when observed intensities of different Raman lines are to be compared, the intensity expression given above refers to a particular mode of vibration of a molecule. When two or three modes are degenerate, each may be shown to have the same intensity, and so, as degenerate modes have the same frequency, the observed intensity of the Raman line will be increased by the factor 2 (or 3) as compared with that for a non-degenerate mode. No attempt is made in this report to treat the quantum theory of Raman spectra. Several excellent references are available and the reader is referred to them. ^{1, 2, 3, 4}

Factors which influence recorded intensities when using laser excitation were examined in detail. The reasons for such an investigation have been summarized by L. A. Woodward.¹ "The theoretical intensity expressions ---- apply strictly to scattering at right angles to the direction of the incident light. In practice it is no easy matter to define the scattering angle exactly, and therefore so-called convergence effects arise. With appropriate experimental arrangements, these may be reduced so as not seriously to affect the significance of the measurements. The theoretical expressions apply to free molecules. Ideally, therefore, intensity determination should be made upon gaseous samples at low pressures; however, this even if not ruled out for other reasons, would mean that the intensities to be measured would be very low. In practice, therefore, most work is done with liquid samples. This introduces a number of complications.

The first is that geometrical-optical effects (reflections and refractions) will occur both at the entry of the exciting light into the sample, and at the emergence of the scattered light from it. These effects will be different for samples of different refractive index and so will complicate the comparison of observed intensities. The second complication is due to so-called internal effects, arising from the fact that both the intrinsic scattering power of a molecule in a liquid and also the effective electric field strength of the exciting light at the position of the molecule will be affected by the surrounding molecules in its immediate vicinity. It is possible to make allowances for geometrical-optical effects, but our present knowledge does not allow for a reliable assessment of internal effects when comparing measured intensities for liquids.

Geometrical-optical effects were studied in this work because the use of small spectral slit widths complicates Raman intensity measurements of laser-excited spectra. The nature of the slit-function correction in medium-resolution laser Raman instruments is discussed and some effects of asymmetric slit-functions on asymmetric and symmetric Raman bands have

been explored. Corrections to bandwidth and band shape for non-ideal slit-functions are obtained from the concept of an intermediate standard which represents the pure slit-function at some limiting spectral slit width. The corrections are applied to the contours of the Raman bands of CCl_4 at 458 cm^{-1} and CH_3OH at 1208 cm^{-1} band is compared to that obtained for the same band on a high-resolution laser Raman spectrometer. A codification of Raman band shapes by means of two shape parameters is discussed, also. The purpose of this section is to point out some experimental difficulties associated with determining band widths and intensities in laser-excited Raman spectra of liquids and to suggest one method for dealing with these difficulties.

To a large extent, all measurements of Raman band shapes have followed the guidelines outlined by Bazhulin *et al.*⁵ For reasons which will become clear, corrections to recorded band contours when using spectral exciting sources such as mercury arcs are not the same as when using laser excitation. The tool which would be ideal for investigating Raman band widths, the Fabry-Perot etalon, is not applicable to low-intensity bands or to broad bands. Therefore, the spectroscopist must still deal with some kind of correction for the instrument function.

In a medium-resolution, laser-excited Raman spectrometer all of the instrumental effects lumped together, e. g. diffraction effects, optical defects, and finite slit widths are non-negligible. However, for such an instrument it is not necessary to examine each of these distorting factors separately in order to determine corrections to the contour of a Raman band of a liquid.

In cases where the half-width of the Raman band is two-to-three times larger than the spectral slit width of the monochromator, the real contour of the band is given by⁶

$$\varphi_K(\lambda) = \frac{1}{2\pi} \int_{-\infty}^{+\infty} \frac{K(u)}{K_B(u)} e^{-i\lambda u} du \quad (1)$$

where $K(u)$ is an integral function of the experimentally-recorded Raman band contour and $K_B(u)$ is a similar function of the recorded contour of the exciting line. Clearly, if the dispersed contour of the exciting line were known, calculations for the corrections of the recorded band shape would be simplified. On the other hand, $K_B(u)$ is a function of the recorded contour of the exciting line, such that

$$K_B(u) = \frac{1}{\sqrt{2\pi}} \int_{-\infty}^{+\infty} k_B(x) e^{iux} dx \quad (2)$$

where $k_B(x)$ is the observed contour of the exciting line. Earlier experiments in cases where minimum spectral slit widths are not so appreciably different from the band width of an exciting line show that the corrections applied to Raman band widths are negligible if it is assumed that the dispersed curve of the exciting line is equivalent to the non-dispersed curve. This condition is not present in a laser-excited spectrum, and the correction to the recorded band width is always mainly the slit function and not the band width of the exciting source. Thus even for well-dispersed, laser-excited Raman bands, not only is the band half-width correction derived primarily from knowledge of the slit function, but also the band wing corrections tend to be too small due to the wide deviation from a dispersed condition of the exciting line. The effect of a finite spectral slit width is non-negligible, then, even though the Raman band half-width might be two or three times larger than the spectral slit width, and this effect is especially pronounced if the Raman band is highly asymmetric.

Bernstein and Allen⁷ as well as Bondarev⁸ have approached Raman band deconvolution from the standpoint of extrapolated symmetric slit functions. In solving an integral equation for true band shape, the slit function is assumed to retain its symmetric character throughout the range of interest. But the asymmetric character of the slit function in a medium-resolution Raman instrument is enhanced, not smoothed, by the narrow band sources of represented by a He-Ne laser, and therefore there is a more complex interaction between the slit function and the relative-intensity-proportional parameters of the Raman band in question. From a practical standpoint, some internal standard of Raman band half-width is needed in order to conveniently compare two Raman bands of liquids. Otherwise, a reference to an absolute intensity standard for band half-width-peak-height measurement would have to be made. The precision obtained by rationing two recorded intensities depends upon the method of deconvolution of the recorded contours, a problem complicated by the widely-varying band widths encountered in Raman spectra of liquids. Thus it is clear that a method must be devised to separate the effect of dispersed and non-dispersed bands.

One method of separating the effects of dispersed and nondispersed bands is to choose an intermediate standard which represents the pure slit function at some limiting spectral slit width. The Neon emission lines at 6505.53 Å and at 6717.04 Å were chosen as convenient intermediate standards for this work because of the spectral positions of these lines near the CCl_4 Stokes 458 cm^{-1} band and the CH_3OH Stokes 1028 cm^{-1} band, respectively, when excited by a He-Ne laser (6328 Å). Also, the intensities of these lines are conveniently low. These two Raman bands were chosen as typical examples of an asymmetric and a symmetric band, respectively.

An experiment was performed at the beginning of this work to determine if the band half-width of the Neon emission lines extrapolated to zero effective spectral slit width compares closely in value to the band half-width extrapolated in the same manner for the laser exciting line at 6328 Å. The two band half-widths do indeed compare closely which determines that the spectrometer sees the same slit function for both the exciting line and the Neon lines.

A Perkin-Elmer LR-1 laser Raman spectrometer equipped with a polarization scrambler was used in these studies, and the minimum theoretical spectral slit width was known to be 2.4 cm^{-1} . A frosted, thoroughly-preconditioned tungsten lamp was used to determine the mechanical slit zero and the spectral sensitivity of the electro-optical system through the spectral range of interest. No unexpected changes in spectral sensitivity of the LR-1 were noted. The linearity of the amplifier system was examined, also.

When a distortion of a band is examined, it is convenient to represent the distortion in terms of a deviation from a symmetrical band shape. Consider a symmetric band -- the locus of the midpoints of the widths of the band, measured at various percent peak heights (for normalization), is a vertical line intersecting the frequency axis at B_c , the band center, a point directly under the band maximum. If for an asymmetric band midpoints of widths are chosen at various percentages of the peak height, the locus of these midpoints extrapolated to zero intensity, $I < \epsilon > 0$, becomes a "symmetry plot." The recorded band is designated B_1 , and the symmetry plot for band B_1 bears some functional relation to a symmetry plot of another band, B_2 , which might be an internal standard for the instrument. This functional relation is determined by the convolution.

If a Raman band, B_2 , such as the 458 cm^{-1} band of CCl_4 is chosen as an internal intensity standard for a particular instrument, then any other Raman band, B_1 , may be compared in such a way that $(\text{peak height})_1 / (\text{peak height})_2$ is a constant for a given ratio of half widths α_1 / α_2 , following the calculation outlined by Berezin et al.¹⁰ For a given slit width $S = A$, the intensity, I_2 , of band B_2 is a convolution of a dispersed Raman band and a non-dispersed exciting line, and the relative intensity, I_1 , of band B_1 is a solution of the convolution between two dispersed curves; so in general the internal standard is a different concept not involving integration with frequency as the independent variable. Thus for band B_2 the product $[(\alpha \text{ corrected})_2 \times (\text{normalized peak height})_2]$ is chosen as the internal standard of band shape at a given slit width. In order to accomplish this standardization for a given slit width it is necessary to do only the following: (a) at $S = A$, normalize the

peak height of B_1 to the peak height of B_2 by recording them at equal amplitudes, (b) read off the half-width corrections from a set of standard curves like Fig. 8 (to be explained), and (c) form the ratio $\alpha_1/\alpha_2 = I$.

The bandwidth at any percent peak height, I , is independent of the ordinate scaling factor, i. e., the gain of the amplifier (if the amplifier is linear). The bandwidth is corrected first to correspond to a frequency interval over which it may be imagined that all frequencies present in the interval are weighted equally with respect to the instrument optical function, which is the meaning of convolution in this context: thus at equal values of intensity the bandwidth of the instrument optical function is subtracted from the bandwidth of the recorded band. If one is interested in band shape in order to characterize various quantities of engineering interest such as source distribution, filtering, etc., then it becomes necessary to adjust the midpoints of each width, corrected first as just described, to the correct energy position in the spectrum, i. e., to an equilibrium position of the true band center unmodified by the fact of distortion due to asymmetric source distribution (Rayleigh line modified by the instrument optical function). This correction is accomplished by the arithmetic operation of displacing laterally (+ or -) the bandwidths at corresponding values of intensity by the amounts which are opposite in sign to the deviation of the center of symmetry of the Rayleigh line. Thus one has displaced energy intervals of a recorded band (which has been corrected for the instrument optical function) by the negative of the incremental energy shifts due to any asymmetry in the instrument optical function.

Interestingly enough, corrections to bandwidth become larger at the band wings which illustrates the difficulty in choosing integration limits for measurements of integrated intensity. For example, even before correction of the 2836 cm^{-1} band of CH_3OH , there is energy which is easily measureable over a range of 157 cm^{-1} . After correction, it is necessary to curve-fit the wings and to use generalized Gaussian quadratures to obtain an estimate of the energy thrown into the wings at a different spectral slit widths. Also, if

bands overlap or if bands lie on top of a high scattering background the choice of the half peak-height is altered by the change in the band contour. The difficulty inherent in choosing what area to include under bands of this type is avoided by observing the behavior of the center of symmetry of the band at successively narrower slits. The correct choice for the half peak-height can be deduced from a family of standard curves even if the band is poorly resolved or if it is on a sloping background.

Many quantitative features of a Raman band should be codified with precision and exchanged among Raman spectroscopists. Band half-width, peak height, and band contour are useful parameters and are relatable to the theoretical models which predict Raman spectra. Different band contours of infrared absorption spectra of gaseous materials are designated conveniently as A, B, and C-type bands, depending upon the band contour. A general classification system for Raman bands is needed, also. Ramsey¹¹ has discussed the factors influencing the intensities and shapes of infrared absorption bands of substances in the liquid phase. For a Raman band of a liquid, however, if instead of the usual frequency interval an interval of intensity is chosen and used to define a factor F which is related to band contour, then an important comparison to an internal standard of Raman band shape may be obtained. One such factor could be defined as

$$F_{1/2} = \frac{\int_{0.1}^{0.5} \nu + (I) dI - \int_{0.1}^{0.5} S(I) dI}{\int_{0.1}^{0.5} \nu - (I) dI + \int_{0.1}^{0.5} S(I) dI} \quad (3)$$

which is the ratio of the areas on either side of the center of symmetry, $S(I)$, and lying in the strip from 10% to 50% peak height. (See Fig. 4). Another factor

$$F_1 = \frac{\int_{0.5}^{1.0} \nu + (I) dI - \int_{0.5}^{1.0} S(I) dI}{\int_{0.5}^{1.0} \nu - (I) dI + \int_{0.5}^{1.0} S(I) dI} \quad (4)$$

expresses the ratio of areas above 50% peak height and lying on either side of the center of symmetry.

CHAPTER II

RESEARCH PROCEDURES

1. Solutions

Experiments were performed to determine the lower limit of detectability of water solutions of CS_2 and C_6H_6 . The solutions tested were prepared by diluting a saturated solution to the desired concentration.

At room temperature (22°C) benzene has a solubility of 0.082 gm per 100 mL of water. The concentrations of a saturated solution is 928 ppm by volume. Dilution by 40-to-1 yields an approximate concentration of 23 ppm.

Benzene is highly volatile at room temperature. Through distillation from the solution during handling and mixing, it is assumed that the actual concentrations are somewhat lower. Even in the closed cell the concentration (as observed by the strength of the 992 cm^{-1} band) decreased with time.

The solubility of CS_2 in water at 50°C is 110 ppm by volume. Diluted 5 to 1, the resulting concentration was approximately 22 ppm.

2. Instrument Function

A collimated beam from the laser was brought into a multipass liquid cell via one reflection from the horizontal. The cell was adjusted such that all energy not lost to scattering or reflection attenuation was returned to the laser output mirror and then dissipated along the return beam inside the cell. This adjustment assured the greatest number of passes and the greatest intensity out of the cell. The vertical plane of the multiple-reflected laser beam within the cell was adjusted along the line of the slit so that the entire slit was filled uniformly. If the cell angle and the laser-entrance-beam geometry is correct, very little self-absorption will affect the intensity measurement and the cell may be standardized in this way for relative scattering-cross-section measurements. The source used for the intermediate standard is a thoroughly-conditioned G. E. Neon glow lamp which was attenuated

to similar detected levels as the Raman bands recorded by using stacked, pre-calibrated, neutral-density Nikon photographic filters of high uniformity. Each Raman band and each Neon line was scanned at various spectral slit widths, adjusting the gain and response of the instrument suitably. Some typical scanning rates were from 0.5 to 2.0 cm^{-1} /minute. Measurements of band widths were made against the chart scale. On the abscissa of the graphically-reduced data, the relative incremental frequency shift is measured from B_c , a point directly under the maximum ordinate of a band. All the data were compared on a scale which bears a linear relation to wave number and to the position of the grating-drive indicator. Individual instruments will have different incremental scales.

CHAPTER III

DATA AND RESULTS

At a concentration of 23 ppm the 992 cm^{-1} band of benzene was recorded on a Jarrell-Ash double monochrometer using a multipass cell, 2.5 ml capacity: 30 mW of laser power enters the cell. At a concentration of 22 ppm the 656.5 cm^{-1} of CS_2 band was detectable. The stability of this concentration was also in question, since the solubility of CS_2 in water decreased with increasing temperature. Due to the heating effect of the laser beam bubbles formed on the sides of the cell within a few minutes of placing the cell in the laser beam.

In Fig. 5 is compared the behavior with slit width of the half-width of the 458 cm^{-1} CCl_4 band with that of the Neon line at 6505.53 \AA . The half-width scale has been normalized to the peak height of the CCl_4 band. A similar comparison is presented in Fig. 6 for the 1028 cm^{-1} CH_3OH band and the Neon line at 6717.04 \AA . In Fig. 7 is displayed at three slit widths the effects of an asymmetric slit function upon the symmetry plot of the CCl_4 band. The corrections to bandwidth for various percentages of the peak height are given for CCl_4 in Fig. 8. The relative correction in this figure is reduced to the same scale as that of the scale $\Delta\nu(B)$ for CCl_4 in Fig. 7. The recorded and corrected band contours of CH_3OH are shown in Fig. 9. This figure is corrected for both bandwidth and band shape distortion.

In Table I is recorded the results of a comparison among three methods of measuring the relative intensities of the 1028 cm^{-1} Raman band of CH_3OH and the 458 cm^{-1} band of CCl_4 . Table II contains ratios of Raman bandwidths at three spectral slit widths for two bands of CH_3OH and for two bands of C_6H_6 . Presented in Table III are $F_{1/2}$ and F_1 , as defined earlier from Fig. 4 for the Raman bands of CH_3OH at 2837 cm^{-1} and at 1028 cm^{-1} .

Illustrated in Fig. 5 are the effects on band half-widths of the interaction of an asymmetric slit function with an asymmetric Raman band. If a

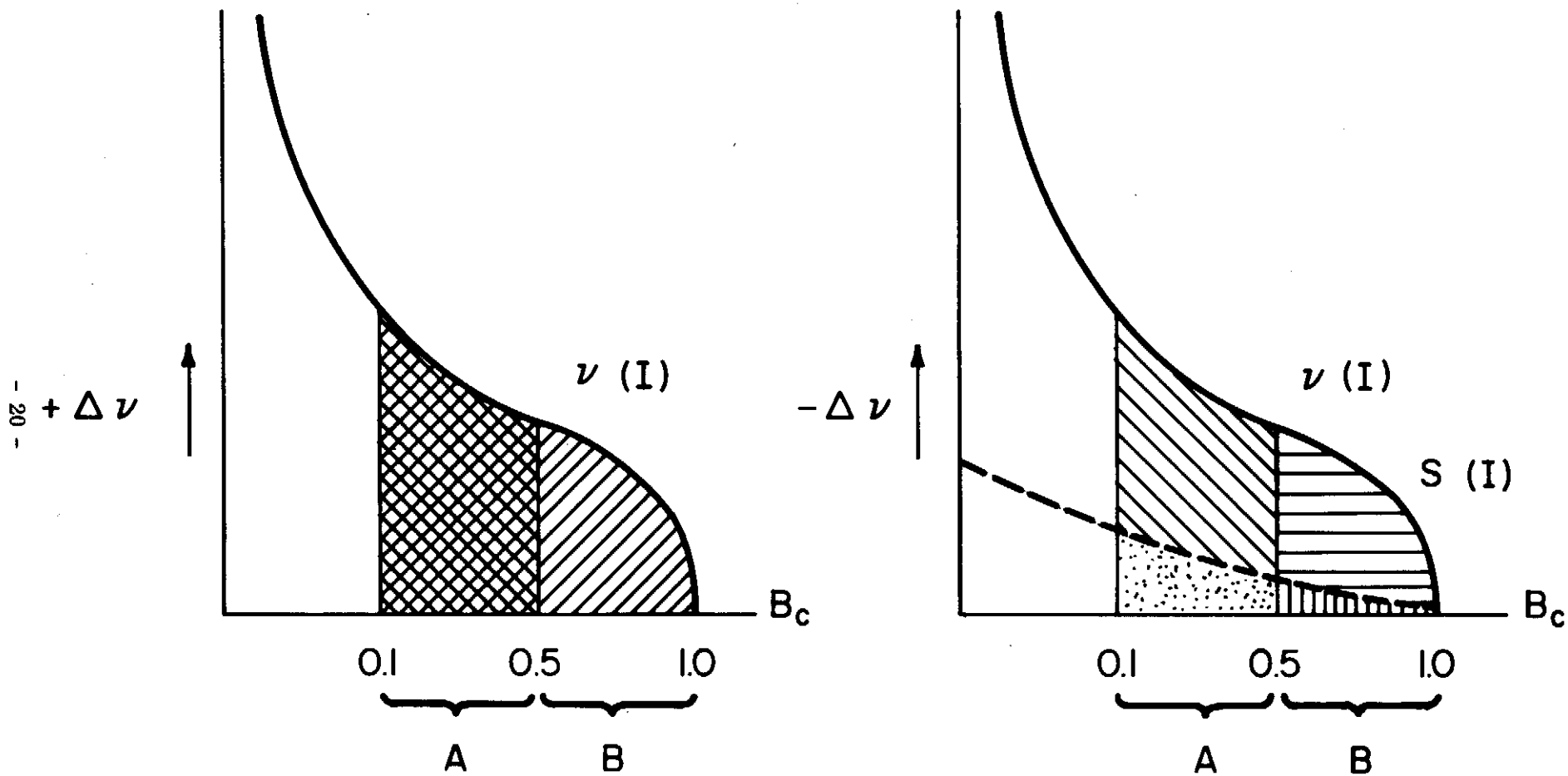


FIG. 4 Sketch of a Hypothetical Raman band Divided Along the Band Center, B_c , for the Purpose of Discussion of the Symmetry Characteristics of the Band in Terms of Area. The Band Contour is $\nu(I)$, and the Center of Symmetry is $S(I)$.

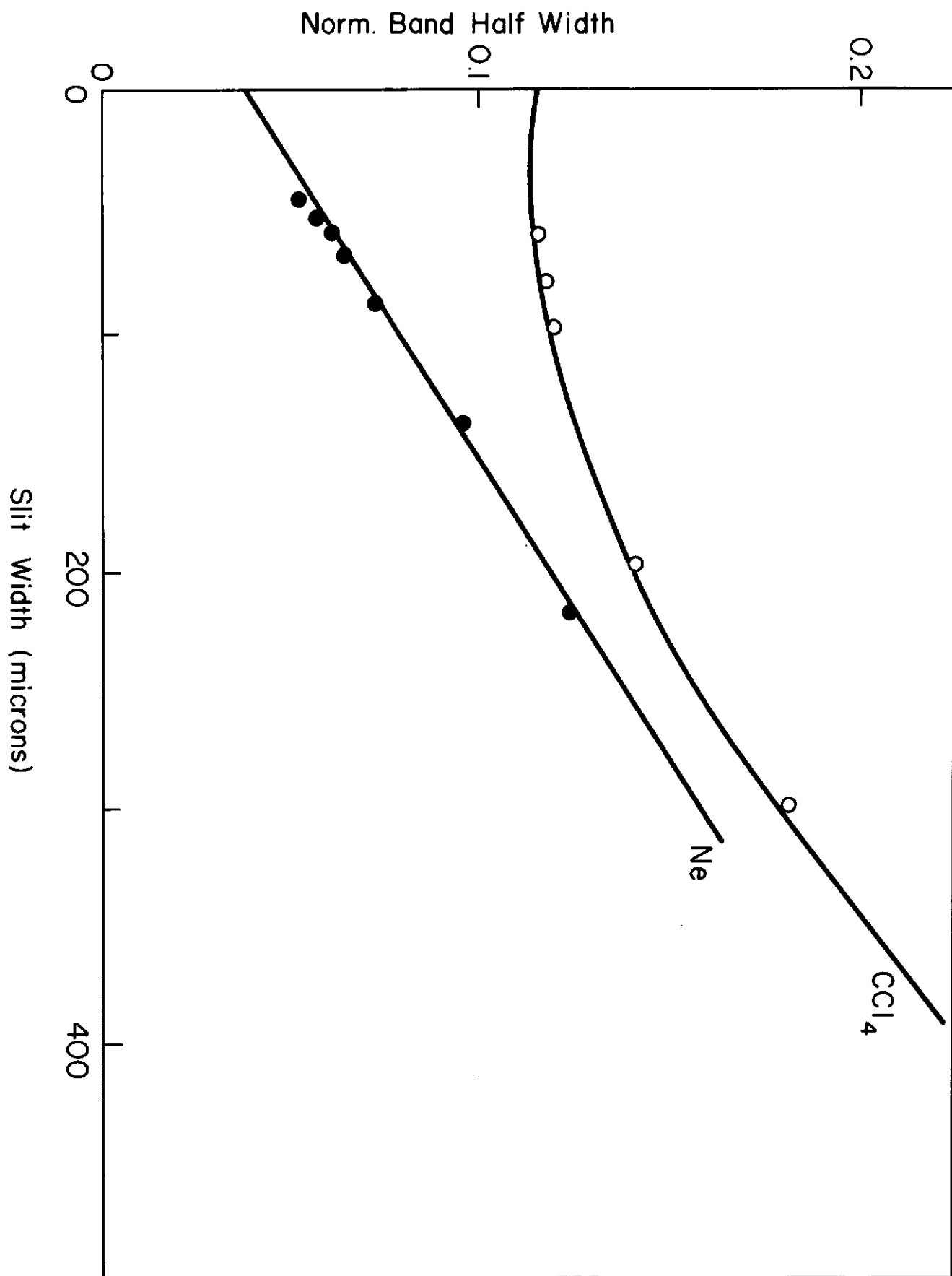


FIG. 5 The Normalized Band Half-Width of the CCl₄ Raman Band at 458 cm⁻¹ and the Neon Emission Line at 6506.53 Å for Various Slit Widths.

TABLE I

A Comparison of Raman Band-Intensity-Proportional Parameters for the 1028 cm^{-1} Raman Band of CH_3OH and the 458 cm^{-1} Raman Band of CCl_4

Method of Intensity Measurement	$I_x(\text{CH}_3\text{OH})$	$I_s(\text{CCl}_4)$	$I_s(\text{CCl}_4)/I_x(\text{CH}_3\text{OH})$
Areas ^{a, b}	2.81	15.93	5.67
Uncorrected half-width times peak height ^b	20.70	115.20	5.57
Corrected half-width times peak height ^{b, c}	20.46	111.60	5.45

(a) Taken with $75\ \mu$ slits

(b) In arbitrary chart divisions

(c) With corrections for the slit-function effect on the band half-width

TABLE II

Ratios of Raman band widths at three spectral slit widths for the ν_2 (2836 cm^{-1}) and the ν_4 (1028 cm^{-1}) vibration of CH_3OH and for the ν_2 (992 cm^{-1}) and the ν_{18} (606 cm^{-1}) vibration of C_6H_6 .

Spectral Slit Width	5 cm^{-1}		3 cm^{-1}		1 cm^{-1}	
	CH_3OH 1028/2836	C_6H_6 606/992	CH_3OH 1028/2836	C_6H_6 606/992	CH_3OH 1028/2836	C_6H_6 606/992
Ratio of band widths						
Percent Peak Height						
50	1.21	1.47	1.24	1.76	1.27	2.77
40	1.17	1.56	1.20	1.92	1.20	2.88
30	1.14	1.63	1.14	2.00	1.15	3.12
20	1.07	1.78	1.12	2.18	1.12	3.33

TABLE III

A codification of two Raman bands of CH₃OH according to F-values

2837 cm ⁻¹				
Frequency Increment	+ Δν	- Δν		F-value
Area A (sq. in.)	$\int_{0.1}^{0.5} \nu^+ (I) dI = 11.84$	$\int_{0.1}^{0.5} \nu^- (I) dI = 11.63$	$\int_{0.1}^{0.5} S(I) dI = 0.11$	$F_{1/2} = 1$
Area B (sq. in.)	$\int_{0.5}^{1.0} \nu^+ (I) dI = 5.11$	$\int_{0.5}^{1.0} \nu^- (I) dI = 5.30$	$\int_{0.5}^{1.0} S(I) dI = 0.05$	$F_1 = 1$
1028 cm ⁻¹				
Frequency Increment	+ Δν	- Δν		F-value
Area A (sq. in.)	$\int_{0.1}^{0.5} \nu^+ (I) dI = 6.16$	$\int_{0.1}^{0.5} \nu^- (I) dI = 8.39$	$\int_{0.1}^{0.5} S(I) dI = 1.17$	$F_{1/2} = 0.53$
Area B (sq. in.)	$\int_{0.5}^{1.0} \nu^+ (I) dI = 3.39$	$\int_{0.5}^{1.0} \nu^- (I) dI = 4.00$	$\int_{0.5}^{1.0} S(I) dI = 0.36$	$F_1 = 0.69$

comparison of slit-function-modified half-widths is made at mechanical slit widths of less than 200 microns (equivalent to a 5 cm^{-1} spectral slit width), it is seen that an undetermined error will be introduced if one assumes the extrapolation of the halfwidth, α , for CCl_4 should be linear. The extrapolated values for α in Fig. 5 are 0.04 for the Neon line and 0.12 for the CCl_4 band, assuming the isotopic components of the band are not resolved. The corrected value of α for the normalized CCl_4 band is, therefore, 0.08. This value compares favorably with 0.10, a normalized value derived from the envelope of the resolved CCl_4 band at 458 cm^{-1} (scanned with a Jarrell-Ash double monochromator, spectral slit width 0.5 cm^{-1}). Because α for the laser exciting line does not enter as a meaningful correction, Fig. 5 serves to give the ratio correction to the intensity for any other Raman band of a liquid relative to the CCl_4 standard band when scanned at any other spectral slit width.

Figure 6 shows for the Raman band of CH_3OH at 1028 cm^{-1} the same type of correction as Fig. 5. The interaction of an asymmetric slit function with this band contour is not as pronounced, and the extrapolation is linear. In Fig. 7 the progressive skewness of the center of symmetry below slit widths of 100 microns means that serious errors in band deconvolution will occur if the slit-function corrections are applied only at band half-widths. These corrections are the errors which would occur at zero-slit extrapolation points if the extrapolation is made without knowledge of the instrument optical function. Figure 8 is constructed from the data in Fig. 7 and from a symmetry plot of the attenuated Rayleigh scattering of CCl_4 which was recorded at the same slit widths as shown in Fig. 7.

A comparison of extrapolations for the band half-widths was made by comparing the LR-1 data in Fig. 9 with the extrapolated halfwidths of the same bands recorded on a Jarrell-Ash Model 25-300 Raman spectrometer. In an earlier paper⁹, the extrapolated halfwidth of the Raman band of benzene at 992 cm^{-1} was reported to be 1.49 cm^{-1} using the techniques described in this paper. The Jarrell-Ash instrument is found to have a nearly symmetric slit function and on this instrument the extrapolated half width for the 992 cm^{-1}

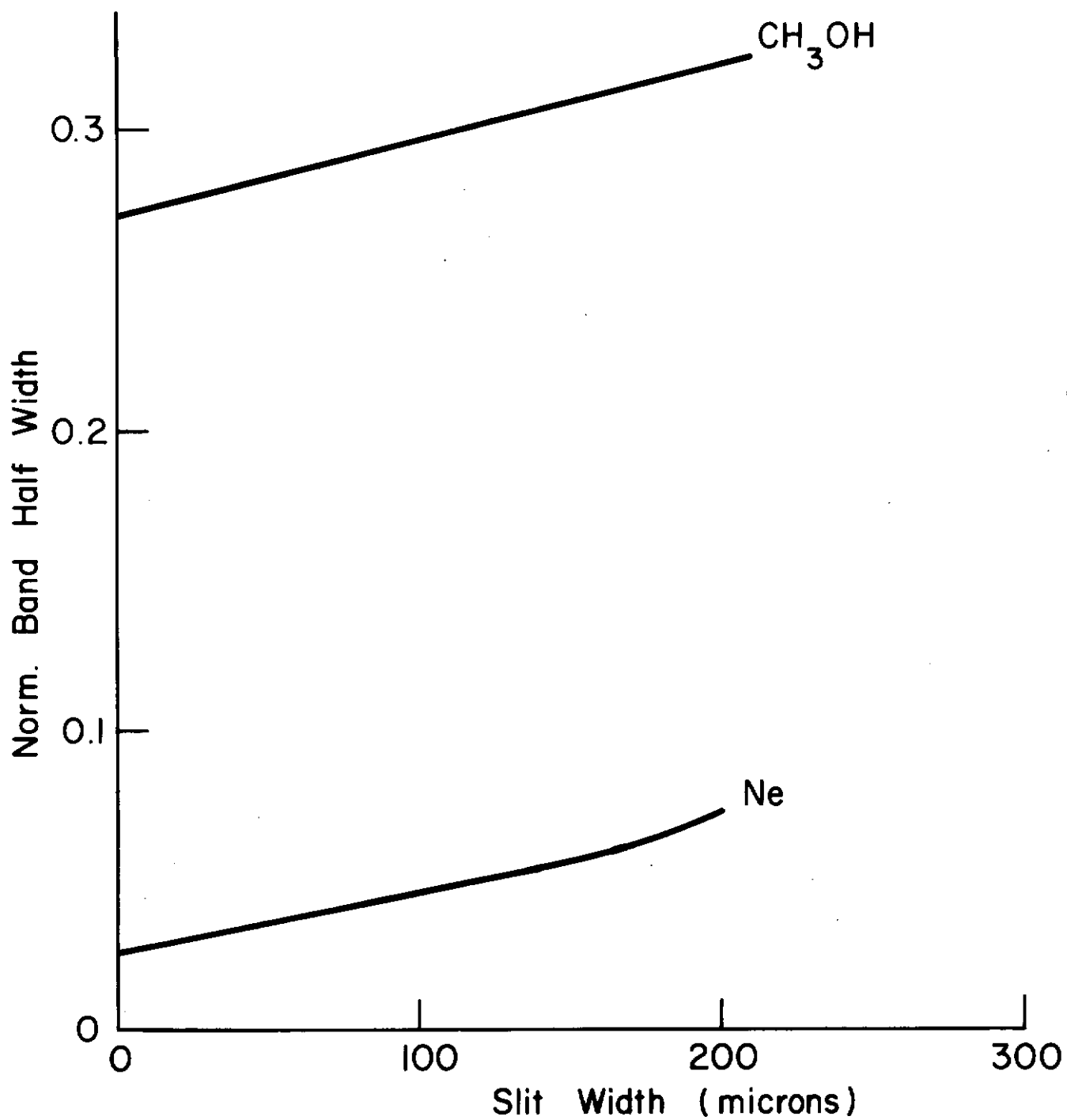


FIG. 6 The Normalized Band Half-Width of the CH₃OH Raman Band at 1028 cm⁻¹ and the Neon Emission Line at 6717.04 Å for Various Slit Widths.

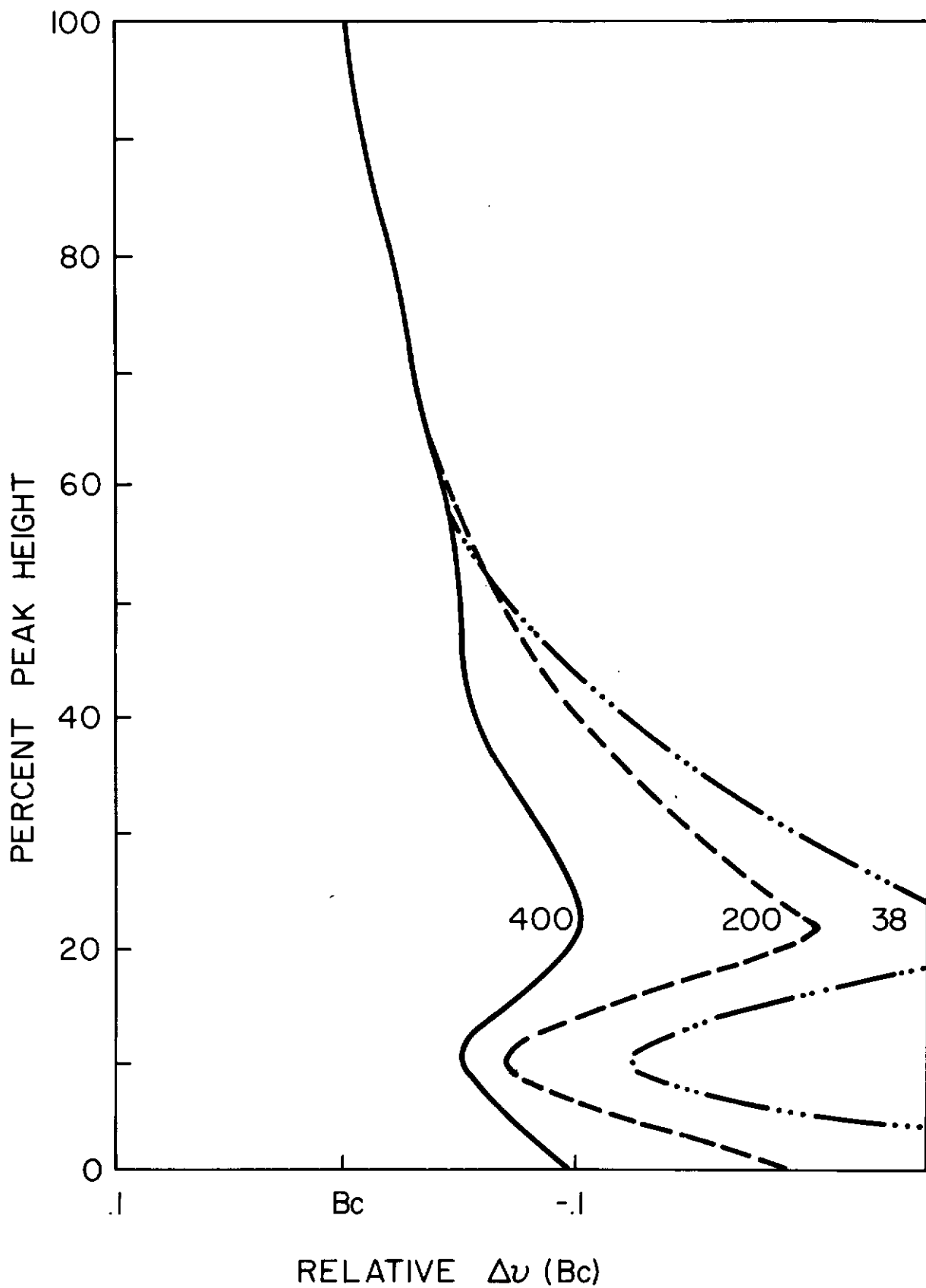


FIG. 7 A Symmetry Plot of the Raman Band of CCl_4 at 458 cm^{-1} for Three Mechanical Slit Widths of the LR-1. The Point B_c is chosen on the Frequency Axis to Lie Under the Peak Height of the Recorded Band. The Fractional Scale on the Abscissa Measures the Deviation of the Center of Symmetry of the Band From that of the Ideal Symmetric Band. Negative Values are Toward Lower-Frequency Raman Shifts, Positive Values Toward High-Frequency Shifts. On this Scale, 0.1 equals 1.3 cm^{-1} .

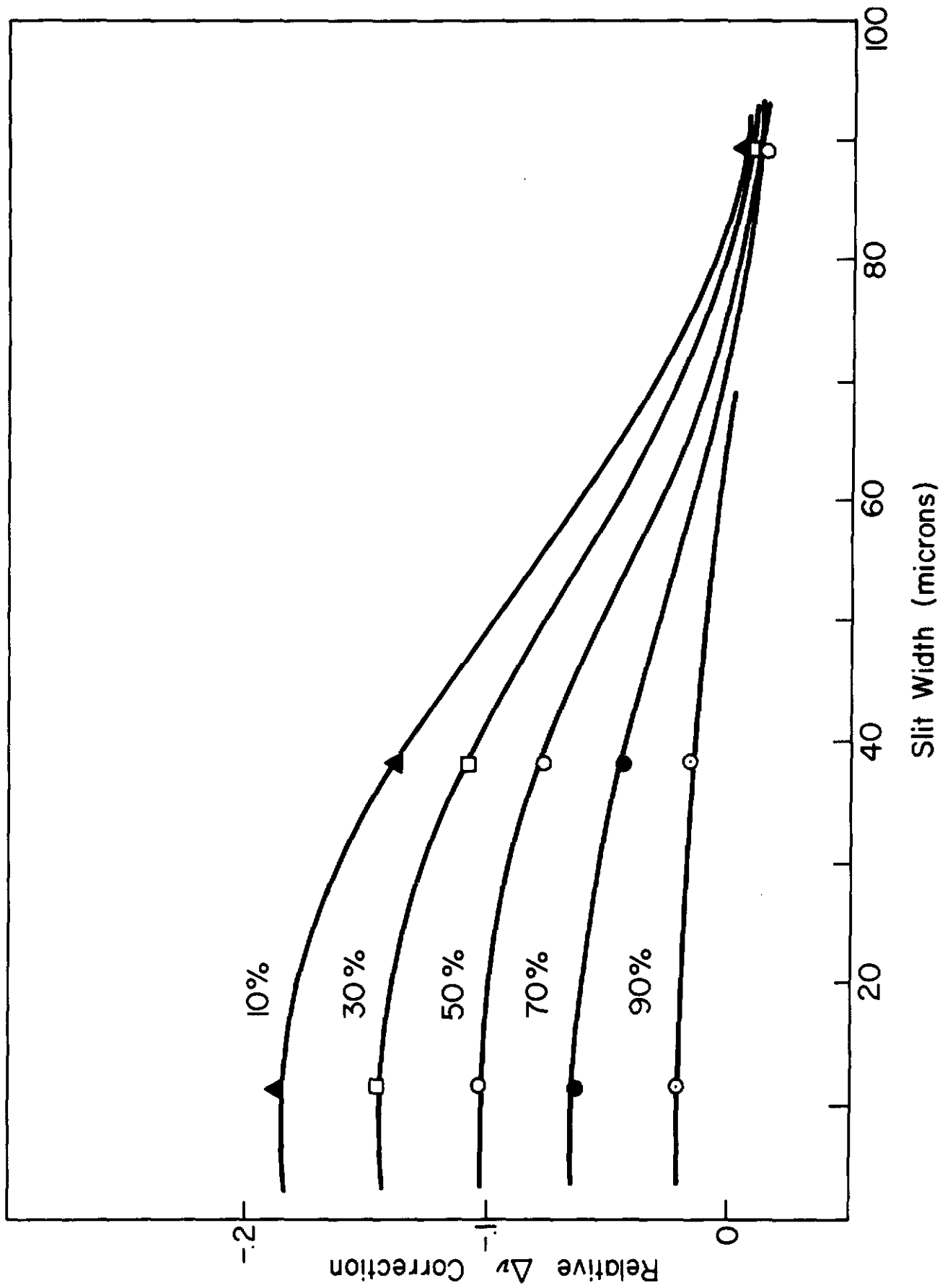


FIG. 8 The Corrections to Widths of the CCl_4 Raman Band at 458 cm^{-1} for Various Percentages of the Peak Height of the Band. The Ordinate is Reduced to the Same Scale as the Symmetry Plots, and the Relative Correction Shown is Added to the Value for B_c .

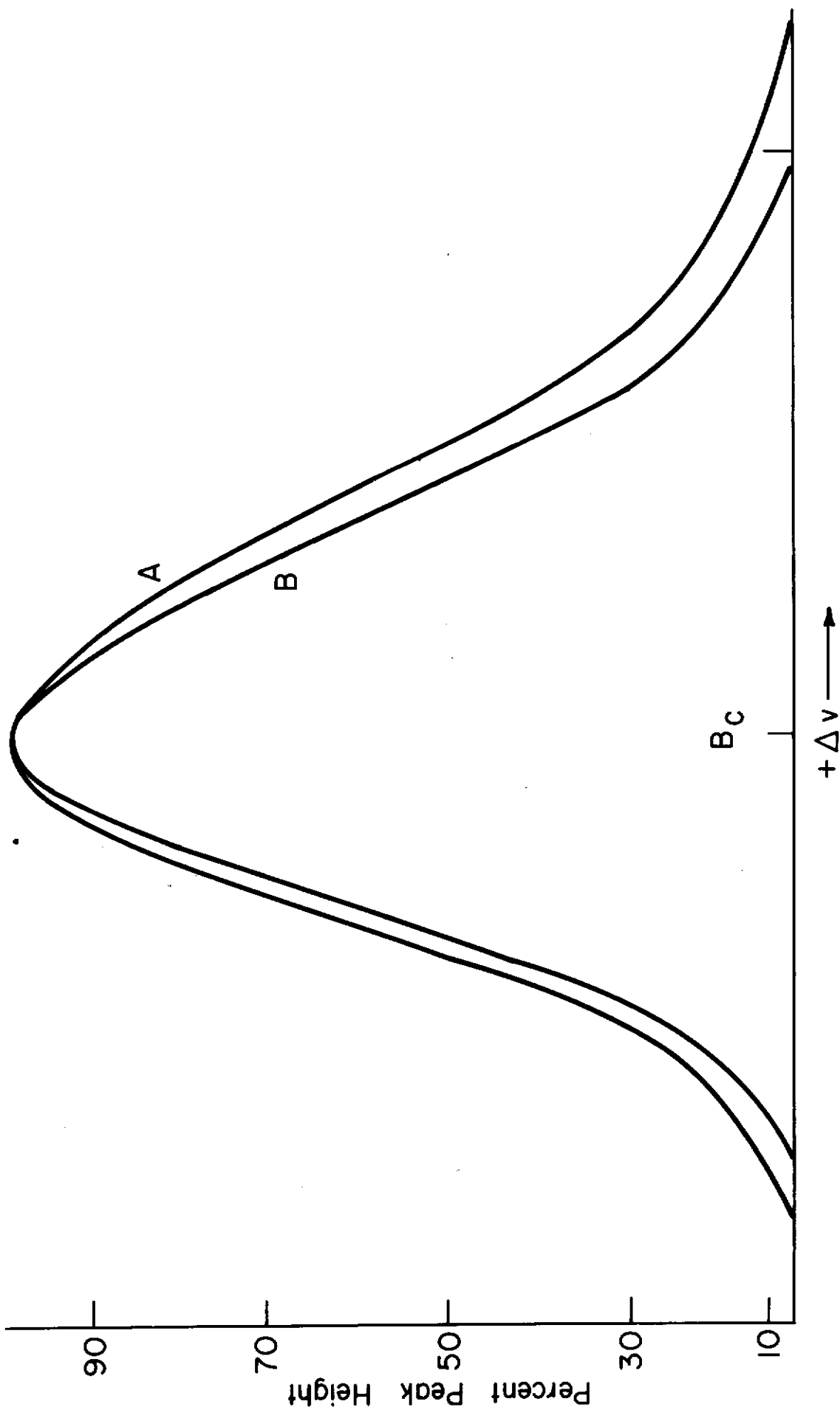


FIG. 9 Result of the Corrections to Bandwidth and Band Shape for the CH₃OH Raman Band at 1028 cm⁻¹. A - Uncorrected; B - Corrected. Slit Width - 50 microns.

band of benzene is 1.50 cm^{-1} . For the 1028 cm^{-1} Raman band of CH_3OH the half-width as determined from the LR-1 data is 26.6 cm^{-1} , while that obtained on the Jarrell-Ash instrument is 25.3 cm^{-1} , about a 5% relative error.

Some additional facts may be learned from Tables I and II. For the convolution of an asymmetric slit function with the CH_3OH band at 1028 cm^{-1} the close agreement of the values in lines two and three, column one, of Table I indicates that it is possible in certain cases to ignore a convolution of this type and to make intensity measurements on the basis of the recorded contour alone. In contrast, the measurements shown in column two for uncorrected and corrected intensity values I_s for CCl_4 differ significantly enough to point out an effect of an asymmetric slit function and a non-dispersed exciting line on an asymmetric band.

The last column in Table I indicates close correspondence between relative intensities measured by either integration or by uncorrected half-width times peak height. A slit width of 75 microns was chosen for the integration-derived value because this slit width is in the transition region where the corrections to the band wings become increasingly important. Experimental methods are lacking for determining the actual transfer of area from under the band into the band wings, and in this transition region band deconvolution would, in certain cases, result in the integrated intensity measured directly from the recording being slightly larger than the corrected value of the intensity; thus the smallest or corrected value of the relative intensity in the last column of Table I is indicative of the change in I_s/I_x to be expected for a corrected integrated intensity measurement. Narrower spectral slit widths may be obtained on the Jarrell-Ash Model 25-300 than on the Perkin-Elmer Model LR-1, so on each instrument was recorded band half-widths and widths below 50% peak height for the 606 cm^{-1} band and the 992 cm^{-1} band of benzene. The widths were ratioed and compared with a similar ratio for the 1028 cm^{-1} band and the 2836 cm^{-1} band of CH_3OH . These bands are suitable for examination of the effect of the convolution of a nondispersed exciting line with a nearly symmetric slit function upon band half-widths which are

well separated in the Raman spectra and which have quite different half-width ratios. (It should be stressed again that the ratios of the half-widths of the benzene bands at the smallest spectral slit widths of the Jarrell-Ash would be affected if the excitation source were to be in a dispersed condition).

In Table II, measured from the spectra recorded on the Jarrell-Ash instrument at 1 cm^{-1} spectral slit width, the ratio of the half-width of the 606 cm^{-1} band to the 992 cm^{-1} band is 2.2 times the ratio of the half-width of the 1028 cm^{-1} band to the 2836 cm^{-1} band. It is seen that for bands with approximately the same half-width (CH_3OH) the changes in half-width ratio is very little with decreasing spectral slit width.

The codification of two Raman bands of CH_3OH according to the F-value discussed earlier, is illustrated in Table III. The quantity $F_{1/2}$ decreases in value as a band becomes more asymmetric, as does F_1 . However, as seen in Fig. 8, the greatest changes in band contour due to convolution occur below 50% peak height, so the ratio $F_{1/2}/F_1$ may be expected to decrease in value as the contour becomes more asymmetric. For the nearly symmetric 2837 cm^{-1} band the ratio $F_{1/2}/F_1 = 1$, but for the asymmetric band at 1028 cm^{-1} the ratio $F_{1/2}/F_1 = 0.77$.

Laser Raman Spectrometer

The basic criterion of the Raman pollution instrument is detectivity. The instrument must be sensitive, but it is the optical signal-to-noise ratio which is finally the limiting factor. In this study an unlimited amount of exciting power is assumed to be available, and therefore the attack has been concentrated on the most efficient way to isolate Raman lines from backgrounds of interfering radiation.

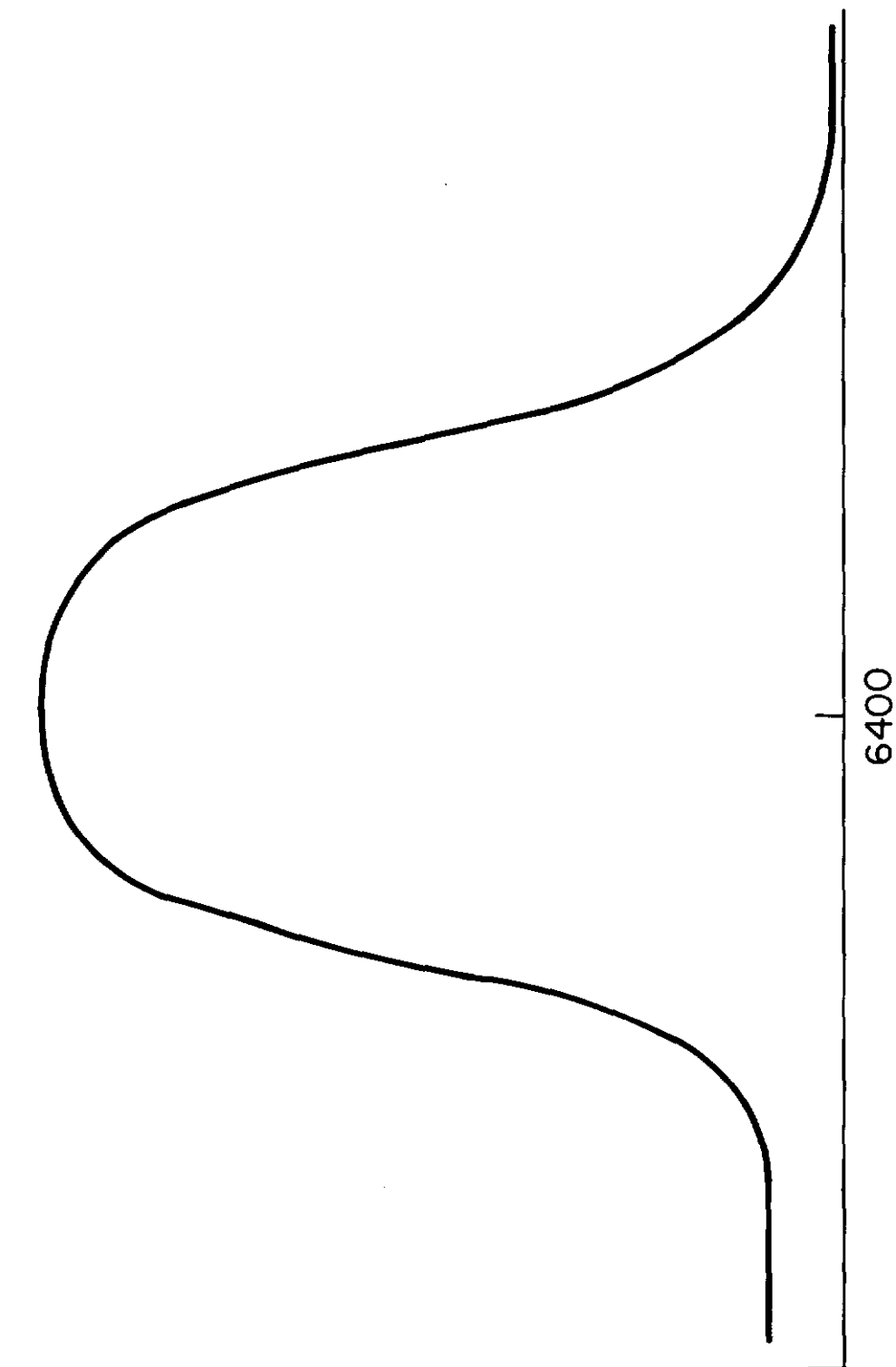
Recently the double monochromator has been in the forefront of instrumentation because the scattered-light background in a double-dispersion or reversed-dispersion double monochromator is nominally a multiplicative factor. That is, one monochromator with a scattered light factor of A^{-x} at some numbers of reciprocal centimeters from the laser line will have a scattered light factor of A^{-2x} if two monochromators are stacked in series,

all other factors (such as spectral slit width) being constant. However, critical in the design of the ideal "double" is the close approach to the Rayleigh line, for this is the region where gain in scattered light factor is to be greatest, falling off rapidly to some constant in the remainder of the useful Raman-scattering region. This characteristic is undesirable from the standpoint of an instrument designed for ultimate detectivity well away from the exciting line and in which the need for spectral resolving power is nil. At present, dispersive and non-dispersive techniques have been combined to build an instrument which will point the proper direction in pollution instrumentation (see Fig. 14).

Excitation radiation from a 50 mw He-Ne laser is chopped at 600 cps by a vibrating mirror chopper which deflects the laser beam across a diaphragm. Noise in the lock-in amplifier is related to the chopping frequency as $1/f$, and 600 cps was chosen as the highest convenient frequency which could be reached with a mechanical chopper and yet take advantage of the improved signal-to-noise ratio. An audio oscillator drives the chopper and provides a synchronizing signal for the lock-in amplifier. A better approach would be to get 100% modulation of the laser but the facilities were not available.

The samples were contained in a standard multipass cell, with the beam making about fifty passes. The Raman and Raleigh scattering was collected and passed to the 1/4-meter Ebert monochromator via the transfer lens system and the 100 Å filter. The 1/4-meter Ebert was equipped with an uncooled photomultiplier, S-1 response, the output of which was fed into a Keithley picoammeter. The output of the DC preamp was then passed to a Princeton lock-in amplifier for signal processing and recovery. The output is the standard 10 mv strip chart recorder.

Several features of this system should be noted. First and most important, the use of the preselecting filter allows the system to operate regardless of the scattered light function of the Ebert because maximum throughput and maximum scattered light rejection occur at the same point in the spectrum. (See Fig. 12). Second, two modes of operation are available.



RELATIVE ENERGY

FIG. 10 Typical Spectral Window Produced by a Band-Pass Filter Which is Tuned by Rotating the Vertical Plane of the Filter With Respect to Radiation Which is Incident Normally. Filter - Oriol Type G-522-6400.

RELATIVE ENERGY

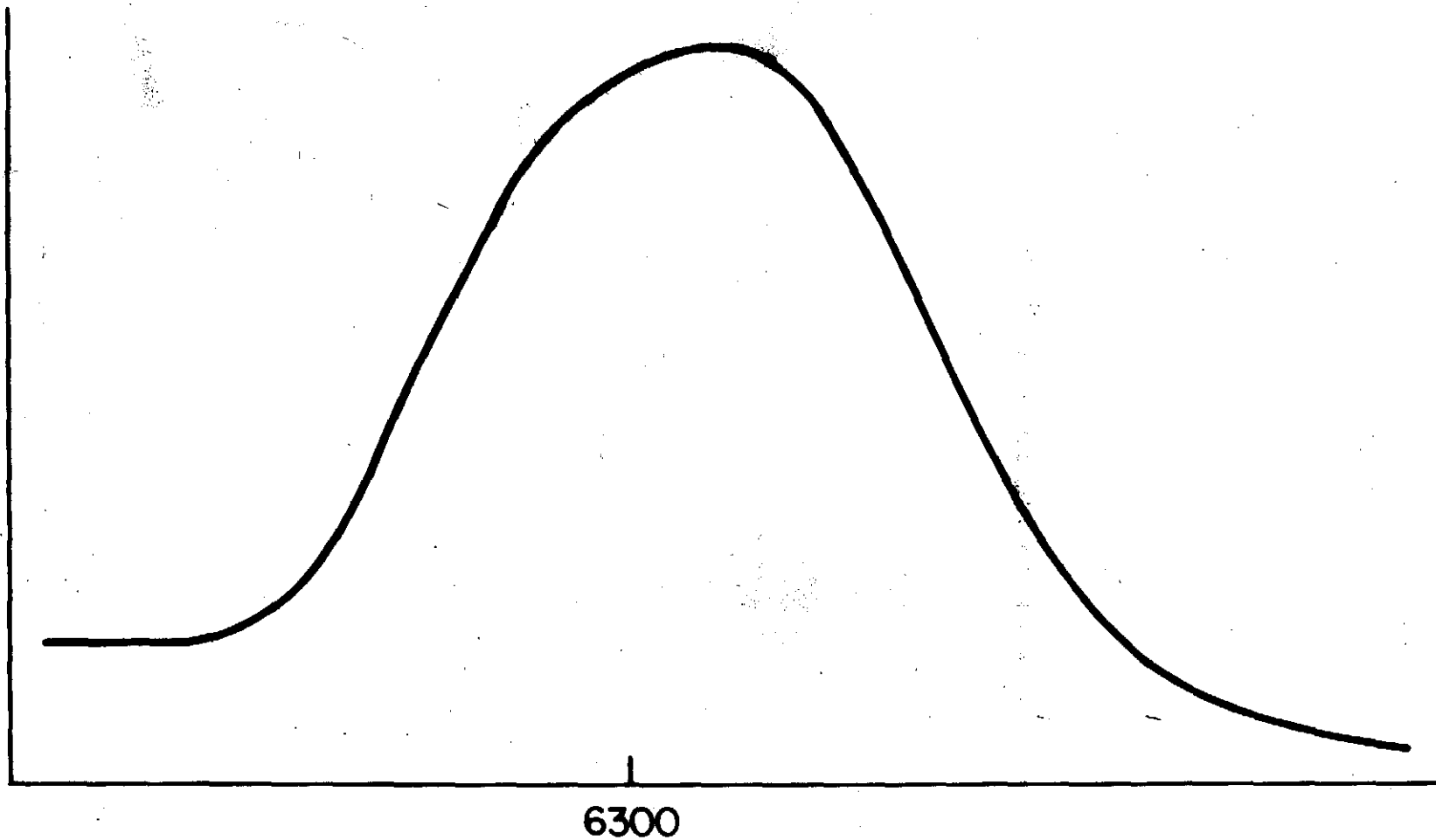


FIG. 11 Spectral Window Produced by the Filter in Fig. 10 (Oriel type G-522-6400) after the Vertical Plane of the Filter is Rotated for Oblique Incidence of the Radiation.

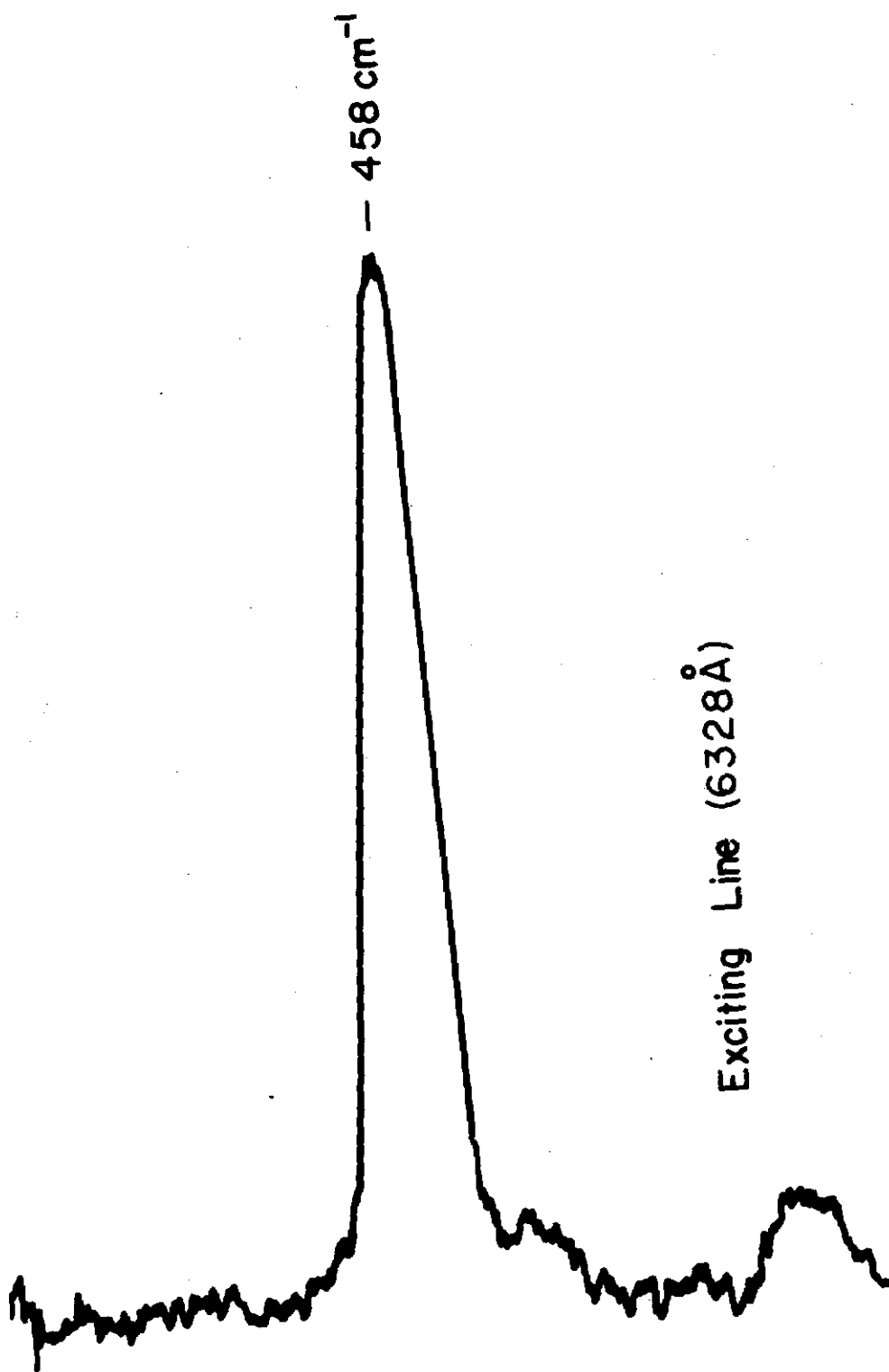


FIG. 12 The 458 cm^{-1} Raman Band of CCl_4 Recorded on the Constructed Spectrometer Using a Band-Pass Filter (Oriel Type G-522-6600); Monochromator is Scanned. Note Relative Amplitude of the Exciting Line.

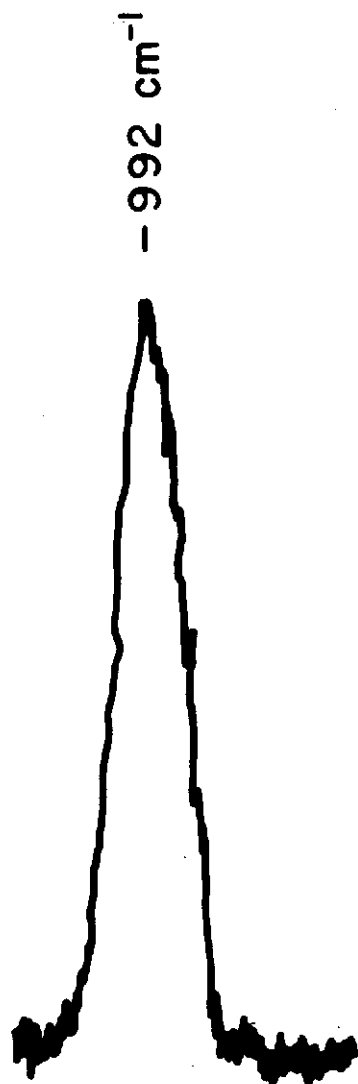


FIG. 13 The 992 cm^{-1} Raman Band of C_6H_6 Recorded on the Constructed Spectrometer Using a Band-Pass Filter (Oriel Type G-552-6800); Monochromator is Scanned.

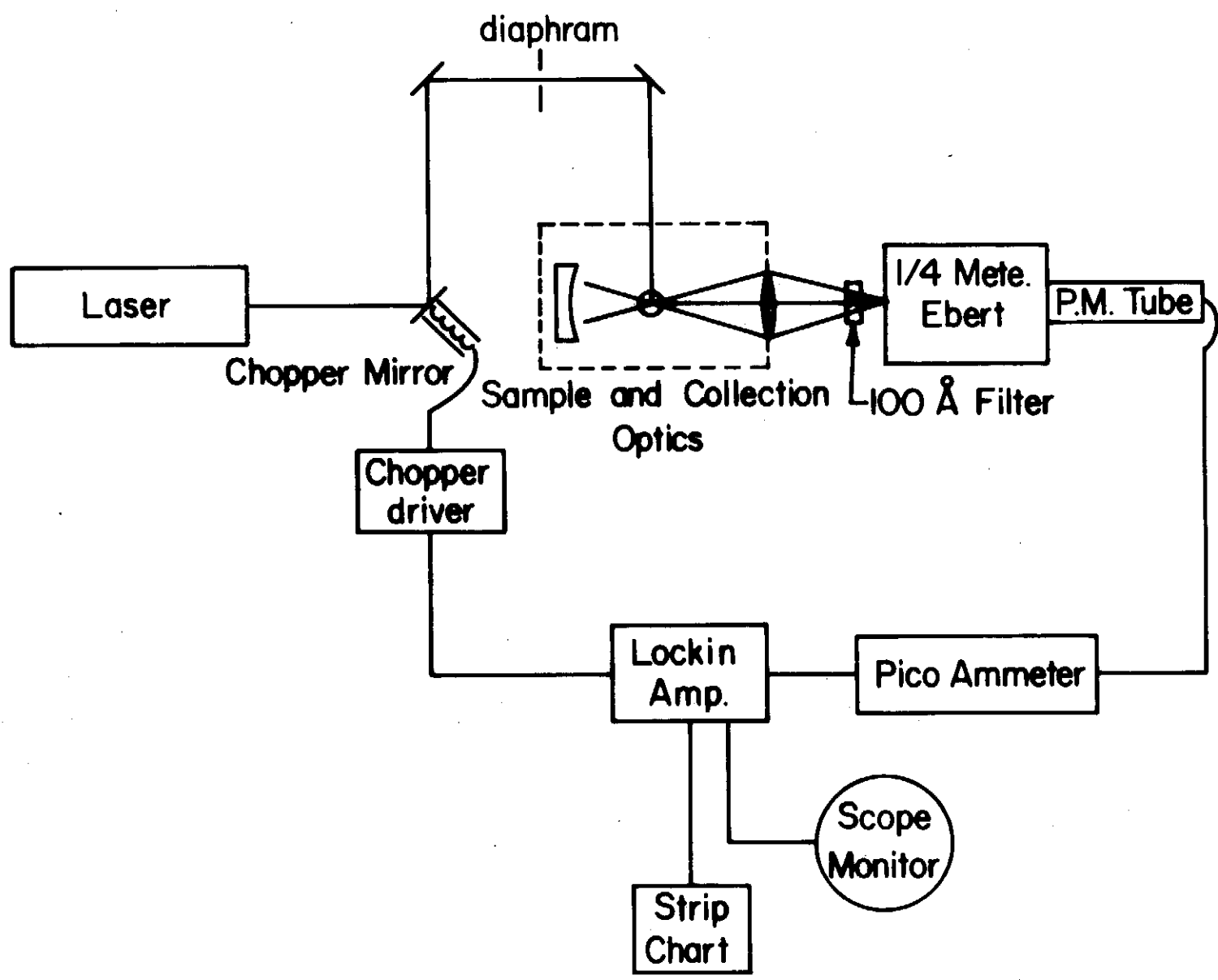


FIG. 14 Block Diagram of a Prototype Laser Raman Spectrometer.

The Ebert may be set at a fixed spectrum point and the window can be scanned, or the window may be fixed and the Ebert scanned as a normal spectrometer system would be. The advantage of scanning the window is that millisecond repetitive scans can be built up on a display with statistical signal correlation techniques. This approach has not been formally undertaken, but commonly two orders of magnitude of signal enhancement could be expected. Third, the use of the high-stability, high-speed picoammeter with current suppression allows operation at high dark current levels, and even though detectivity would be enhanced by nearly 10^2 if the photo-multiplier tube were cooled, the cost and inconvenience for portable equipment must be considered.

The ultimate detectivity of the instrument which is shown in Fig. 14 was found to be approximately 1000 ppm based on an observation of a standard solution of benzene in water, and with an incident average laser power of about 20 mw. An ion laser supplying 1 w could, coupled with other improvements, yield detectivities in the range of 1 ppm for such an instrument.

CHAPTER IV

CONCLUSION

Laser Raman spectroscopy can become a primary tool for the detection of molecular pollutants in water. High-power ion lasers should be used whenever possible. Relatively inexpensive laser Raman spectrometers may be constructed for field use. Such an instrument has a detectivity which is comparable to more expensive Raman spectrometers, but the cost is reduced by a factor of two to four.

Simple arithmetic corrections to bandwidth and band shape can be applied to the contours of laser-excited Raman bands obtained on a medium-resolution instrument. The results are comparable in many cases to the quality of the information obtainable on a high-resolution instrument, and a simplified means of intensity standardization is achieved with a minimum of complex data-reduction techniques by defining the "standard band" for a given instrument. Such progress as is made suggests the pragmatic approach to half-width-shape classification of bands which will be necessary if Raman spectroscopy is to compete with infrared in the analytical areas of spectroscopy where meaningful data retrieval is of paramount importance.

REFERENCES

1. Szymanski, H. A. (ed.), Raman Spectroscopy, Theory and Practice, Plenum Press, New York, (1967).
2. Marcuse, D. Engineering Quantum Electrodynamics, Harcourt, Brace and World, Inc., New York, (1970).
3. Colthup, N. B.; Daly, L. H.; Wiberley, S. E., Introduction to Infrared and Raman Spectroscopy, Academic Press, New York, (1964).
4. Herzberg, G., Infrared and Raman Spectra, D. Van Nostrand Co., Inc., (1945).
5. P. A. Bazhulin, S. G. Rauthan, A. I. Sokolovskaia, and M. Sushchinskii, Soviet Phys. - JETP 2, 663 (1956).
6. See Reference 5.
7. H. J. Bernstein and G. Allen, J. Opt. Soc. Am. 45, 237 (1955).
8. A. F. Bondarev, Opt. Spectry. (USSR) 8, 510, (1961).
9. See reference 4.
10. V. I. Berezin, M. A. Kovner, and B. A. Medvedev, Opt. Spectry. (USSR) 23, 32 (1967).
11. D. A. Ramsey, J. Am. Chem. Soc. 74, 72, (1952).

LIST OF PUBLICATIONS RESULTING FROM THE PROJECT.

1. On the Exploitation of Laser Raman Spectroscopy for Detection and Identification of Molecular Water Pollutants, Water Research, 4, 125 (1970).
2. Slit-Function Corrections Applied to Laser-Excited Raman Bands of Liquids, Applied Spectroscopy, No. 25, 614, (1971).